The thermal impedance spectroscopy on Li-ion batteries using heat-pulse response analysis

Evgenij Barsoukov

(금호석유화학(주))

The thermal impedance spectroscopy on Li-ion batteries using heat-pulse response analysis

Evgenij Barsoukov, Jee Hwan Jang, and Hosull Lee

Kumho Chemical Laboratories, Korea Kumho Petrochemical Co., Ltd, P.O. Box 64, Yuseong, Taejeon 305-600, Korea

Abstract

Novel characterization of thermal properties of a battery has been introduced by defining its frequency-dependent thermal impedance function. Thermal impedance function can be approximated as a thermal impedance spectrum by analyzing experimental temperature transient which is related to the thermal impedance function through Laplace transformation.
In order to obtain temperature transient, a process has been devised to generate external heat pulse with heating wire and to measure the response of battery. This process is used to study several commercial Li-ion batteries of cylindrical type. The thermal impedance measurements have been performed using potentionstat/galvanostate controlled digital signal processor, which is more commonly available than flow-meter usually applied for thermal property measurements.

Thermal impedance spectra obtained for batteries produced by different manufactures are found to differ considerably. Comparison of spectra at different states of charge indicates independence of thermal impedance on charging state of battery. It is shown that thermal impedance spectrum can be used to obtain simultaneously thermal capacity and thermal conductivity of battery by non-linear complex least-square fit of the spectrum to thermal-impedance model.

Obtained data is used to simulate a response of the battery to internal heating during discharge. It is found that temperature inside the battery is by one-third larger that on its surface. This observation has to be considered to prevent damage by overheating.

Key-words:
Thermal impedance spectrum, thermal capacity, thermal conductivity, battery, heat pulse

1. Introduction

As batteries were primarily employed in low-power applications, the question of thermal properties of battery was not relevant to the application design and therefore has not been a subject of extended research. This has been drastically changed with the onset of new high power applications of batteries, such as portable computers, video-cameras, power-tools and hybrid electric vehicles. As the charge/discharge rates used in such devices can reach 15C rate (full discharge within 4 minutes), substantial heat development can occur in a short time and advanced heat-management of batteries becomes important particularly for large batteries or battery stacks to prevent overheating damage or thermal runaway [1]. Later consideration is particularly relevant to Li-ion batteries capable of explosion and fire if overheated. Require-

ments of the engineering of high-power battery systems have resulted in increased attention to the area of modeling the thermal [2-4] and combined electrochemical-thermal [5,6] behavior of batteries. Experimental values of thermal conductivity and thermal capacity of each particular battery type have to be known for such modeling. Thermal properties of many battery components have been studied using the guarded heat flow-meter by Song et al. [7, 8]. Theoretical calculation of thermal conductivity and capacity of a particular electrode stack of Li-polymer battery are given for example in [4]. Such calculation is only possible if the composition of battery stack is known exactly. However, this information is often available only for battery manufacturers. Further problem arises from the fact that thermal characteristic of stack components can be changed after exposure to electrolyte and formation cycle. *In-situ* measurement of these characteristics would give more precise information. Several recent papers provided experimental data on thermal capacity of the cells, measured by calorimetric technique [9,10]. However, no *in-situ* measured experimental data on thermal conductivity of Li-ion batteries is known to us up to date.

In this work we present a new method to measure both thermal conductivity and capacity of a battery simultaneously employing commonly available to electrochemist equipment and without use of calorimeter. The new method adopts the concept of thermal impedance as a complete characteristic of system's thermal properties. Such approach was employed before in different areas [11-13]. The method of measuring the thermal impedance using Laplace transformation of temperature response transient to external or internal heat pulse is described in detail. To justify the new method experimentally, thermal impedance spectra of cylindrical Li-ion batteries of 18650 type made by different manufacturers have been obtained. Especially, the dependence of thermal impedance on state of charge was investigated for Panasonic Li-ion battery. Specific thermal capacity and conductivity were obtained for all batteries using non-linear fit of the thermal impedance spectra to a model impedance function in frequency-domain, developed for the case of cylindrical rod with interfacial heat development.

2. Derivation of thermal impedance functions

Thermal capacity and thermal conductivity can be obtained by a direct analysis of temperature transient, which is measured after applying a heat pulse. Such analysis could be performed, for example, by fitting time-domain experimental data to a model function. However, fit of time-domain data is often not practical, when the system is so complicated that its response can not be described analytically and has to be calculated numerically using considerable computing resources. When some unaccounted thermal time-constants are present in the system, the fit to a beforehand-defined model function will not give indication about their presence or their nature. An alternative approach to analyze circuits with unknown structure is adapted in electronics. Representation of circuit's transfer function as a frequency-domain spectrum allows to obtain parameters for all known elements of the circuit while detecting all unexpected elements in case they are present.

The complex transfer function F(s,x) defined in Lapace domain is commonly derived in an intermediate step for the temperature transient calculation by Laplace method. If a small temperature change is assumed, time domain transients can be derived as $T(t)=L^{-1}\{F(s,x)\}$, where L^{-1} is inverse Laplace transform, s complex frequency $2\pi f i+b$, f frequency, i imaginary multiplier, b is arbitrary real number, and x – space coordinate. Such functions have been derived for large variety of shapes of the heat conductors and heat application boundaries as solutions of *subsidiary equations* [14].

Exploiting the mathematical analogy between the formalisms describing linear time-invariant electrical networks and thermal conductors, we can represent F(s,x) as a product of two functions I(s) and Zt(s,x). Here the first function is the Laplace transform of heat excitation and the second is a complete description of thermal properties of the system, dependent on thermal conductivity, thermal capacity and shape of thermal conductor.

When the function Zt(s,x) is known, in a special case when b=0 and space coordinate is fixed, Zt($2\pi f^*i$) is mathematically analogous to electrical impedance and is called here "thermal impedance function". In contrast to time-domain response functions, thermal impedance functions have in most cases analytical expressions. Those functions can be evaluated for a set of given frequencies f_i as a set of complex numbers Zt_i representing a thermal impedance spectrum. The thermal impedance spectrum can be visualized similarly to an electrical impedance spectrum in a complex plot. The spectrum in such presentation gives indications about contributions of different parts of the system to heat transfer and allows detecting the relative changes of thermal properties even by simple visual observation. Thermal resistance and thermal capacitance can be geometrically deduced from the spectrum in a complex plot. For example the the value of serial resistor can be obtained from highest frequency point of the spectrum and of value of parallel resistors – from the diameter of the semicircle.

Due to the mathematical similarity to the electrical model, thermal impedance functions can be derived similarly to electric impedance functions, essentially using Ohms and Kirhofs laws. In this approach heat flow is treated as current equivalent and temperature gradient as voltage equivalent. Accordingly, thermal resistance can be defined through traditional specific thermal conductivity κ as $R_T=l/\kappa A$ (K s/J) and thermal capacitance through volume-specific heat $C_T = cAl$ (J/K). Here A is the cross-section and l is the length of elementary heat conduction region.

In analogy with corresponding electric components, the complex impedance of these components are $Z(R_T)=R_T$ and $Z(C_T,s)=1/C_T s$ where s is the complex frequency $2\pi fi$. Calculation of complete thermal impedance function of a thermal conductor can be performed by setting up an "equivalent thermal circuit" and by applying the same rules as for electric elements to find the complete impedance between two desired points of the circuit.

Let us consider a case of a thin plate with thickness *l* with specific heat c, exposed to air so that thermal conductivity per unit surface due to radiation cooling is k, being internally heated. The temperature response is measured by thermocouple on the surface. Thermal equivalent circuit will be thermal resistor $R_{rc}=1/\kappa A$ in parallel with thermal capacitor $C_C=cl A$. Thermal resistance of the thermocouple can be accounted as serial thermal resistance R_{ser}. Such model gives a good description of thermal behavior of battery casing and heating coil. Thermal impedance of this model is given by Eqn. 1

$$Z(s) = \frac{1}{\frac{1}{R_{rc}} + C_c \cdot s} + R_{ser}$$

Eqn. 1

Treatment of the function in terms of thermal resistance and capacitance allows to use impedance fitting software, commonly used in electrochemistry, such as MEISP developed by Kumho Petrochemical Co. Ltd. for analyzing thermal impedance spectra, and then converting obtained parameters into specific thermal values.

In many cases, an impedance function for an electric equivalent circuit is known and can be applied for thermal conduction model. For example, the thermal equivalent circuit for

a setup, where a constant heat flow is applied to one side of a slab and another side is thermally insulated, is equivalent to open-circuit terminated transmission line in electronics. Its impedance function is already known as

$$Z(s) = \sqrt{\frac{R_T}{C_T s}} \cdot coth\left(\sqrt{R_T \cdot C_T \cdot s}\right)$$

Eqn. 2

This equation (divided by factor of two) expresses thermal impedance of prismatic battery to which heat pulse is applied from two opposite wide sides, and where heat flow through its thin sides can be neglected.

Thermal model for cylindrical battery, with heat excitation applied from the surface and with negligible heat flow over the sides, is analogous to diffusion model developed for infinite cylindrical rod. Its impedance function has been derived as a solution of the *subsidiary equation* in [14] and as an electrochemical impedance for diffusion towards the center of cylindrical rod in [15].

$$Z(s) = \frac{I_0\left(\sqrt{2 \cdot R_T \cdot C_T \cdot s}\right)}{\left(\sqrt{2 \cdot R_T \cdot C_T \cdot s}\right) \cdot I_1\left(\sqrt{2 \cdot R_T \cdot C_T \cdot s}\right)} \cdot R_T$$

Eqn. 3

Here I_0 and I_1 are Bessel-functions of the first kind, with 0 and 1 order correspondingly. Note that transformation from cylindrical coordinate system to Cartesian system is required to calculate specific thermal conductivity and capacity from R and C obtained from fit. The application of the transformation results in equations for specific thermal values, given below:

$$k = \frac{1}{2 \cdot \pi \cdot l \cdot R}$$

$$c = \frac{C}{\pi \cdot r^2 \cdot l}$$

Eqn. 4

Here r is the radius of a battery and l is its length.

In addition to cylindrical thermal conductor which represents the bulk of battery's electrode stack, thermal capacity of battery casing together with heating coil C_c and thermal resistance between the casing and electrode stack R_c should be included in the thermal model. When the battery surface is exposed to air, heat flow through radiation and convection has to

be considered. Using thermal circuit approach, it is easily done by adding a "thermal resistor" R_{rc} in parallel to the impedance in Eqn. 3. It can be recalculated to give commonly used *heat transfer coefficient* $\boldsymbol{h}$ as $h=1/(R_{rc}\, 2\pi\, r\, l)$.
Additionally, thermal resistance between the surface and the thermocouple should be considered as a serial thermal resistance. Complete thermal equivalent circuit corresponding to cylindrical Li-ion battery is shown in Fig. 1 .

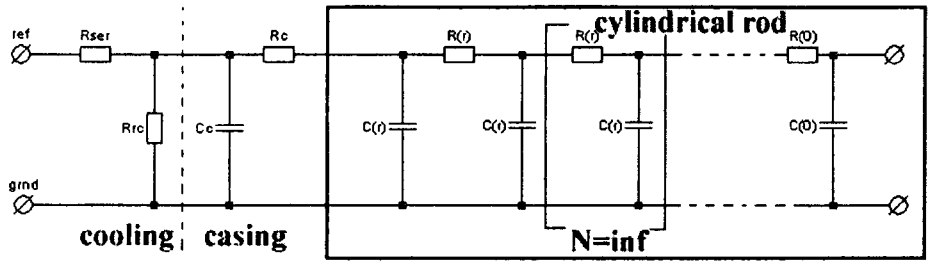

Fig.1
Thermal equivalent circuit corresponding to cylindrical battery heated from the surface under radiation cooling condition

Thermal impedance function corresponding to the circuit is given in Eqn. 5

$$Z(s)=\left[\frac{1}{\dfrac{I_0\left(\sqrt{2\cdot R_T\cdot C_T\cdot s}\right)}{\left(\sqrt{2\cdot R_T\cdot C_T\cdot s}\right)\cdot I_1\left(\sqrt{2\cdot R_T\cdot C_T\cdot s}\right)}\cdot R_T+R_c}+\frac{1}{R_{rc}}+C_c\cdot s\right]^{-1}+R_{ser}$$

Eqn. 5

3. Measurement of thermal impedance spectrum

Thermal impedance function can be obtained directly from time-domain response to heat excitation without any presumption about internal structure of the circuit as given below.

$Zt(s)=L\{T(t)\}/L\{i(t)\}$

Eqn. 6

Here L{} denotes Laplace transform, T(t) is temperature response function and i(t) is excitation function in time domain. For example if i(t) is heat pulse, it can be expressed as heat-flow amplitude I_0 J/sec multiplied by Heavisde step-function $\Phi(t)$ defined as 0 if $t<0$ and 1 otherwise, $i(t)=I_0\,\Phi(t)$. Its Laplace transform can be easily calculated as $L\{I_0\,\Phi(t)\}=I_0/s$.

On the other hand, analytical form of T(t) is generally not known. Information about it is obtained from an experiment as a set of time-dependent samples T_i collected with time interval δt during sampling period Δt. The information about function $Zt(2\pi fi)$ is valid in a frequency range defined by the sampling period and interval. Quantitatively the validity

boundaries are given by Nuquist theorem, $f_{max}=1/2t$ and $f_{min}=1/\Delta t$. Straightforward way to calculate the impedance spectrum based on such set of samples includes interpolation of the samples with piecewise-linear or other functions, followed by numerical integration of resulting function to evaluate the transform integral in Eqn. 7 for $s = 2 \pi f i+b$ with frequency f ranging from f_{max} to f_{min}, while b is chosen so that integral converges. Different methods to define b and resulting approximated solutions of transform integral were proposed in [16-18]].

$$F(s)=\int_0^{\infty} f(t)\cdot e^{-s\cdot t}\,dt$$

Eqn. 7

Numerical integration and selection of optimal *b* can be avoided by using analytical Laplace transform of piecewise-linear function. However, all methods based on interpolation and direct use of Eqn. 7 are quite sensitive to noise which is commonly present when T_i are acquired in experiment, and gives unacceptable results at usually attainable noise level, as shown in [19]. Alternatively, conversion can be accomplished by fitting of experimental data to a physically relevant function having sufficient degrees of freedom to describe all possible system responses. Obtained parameters can be substituted into analytical expression of Laplace transform of such function. Such procedure called *carrier function Laplace transform* (CFLT) is found in [19] to exhibit superior noise-rejection capability. CFLT is therefore used here to calculate L{T(t)} which is then used to obtain the thermal impedance spectrum. Sum of adaptively chosen number of exponents given in Eqn. 8 is used as carrier function in this case.

$$f(t)=\sum_{i=0}^{n} k_i\cdot e^{-\frac{t}{\tau_i}}$$

Eqn. 8

Its Laplace transform is given in Eqn. 9 below.

$$F(s)=\sum_{i=0}^{n} \frac{k_i}{\left(s+\frac{1}{\tau_i}\right)}$$

Eqn. 9

Once the function parameters k_i and τ_i are obtained from fit of the experimental temperature transient, thermal impedance can be calculated combining equation Eqn. 9 with Eqn. 6 as given below:

$$Z(s)=\frac{s}{I}\cdot\sum_{i=0}^{n} \frac{k_i}{\left(s+\frac{1}{\tau_i}\right)}$$

Eqn. 10

here I (W) is the magnitude of the heat flow applied to the surface of the heat-conductor under test at time 0, and s is 2 π f i where frequency f can be selected between 1/δt to 1/Δt.

4. Experimental setup

To demonstrate applicability of the proposed method in real experimental environment and to obtain thermal impedance spectra of Li-ion batteries, we used our proprietary potentiostat/galvanostat with digital signal processor (DSP) for signal generation and data acquisition. The system has been developed by Kumho Petrochemical Co., Ltd. under the name BPS 1000FL Powergraphy Battery Parameterization System.
Cylindrical Li-ion batteries of 18650 type with specified capacity 1500mAh, manufactured by Sony, Panasonic, LG, and Samsung have been obtained from commercial battery packs. Detailed characteristics of those batteries are given in Table 1.

Manufacturer	Radius/height (cm)	Weight (gm)	Discharge capacity (mAh)
Moly Energy	0.9 / 6.5	42.72	1836
Panasonic	0.9 / 6.5	39.47	1536
Hitachi	0.9 / 6.5	41.57	1263
Samsung	0.9 / 6.5	40.93	1436

Table 1
Characteristic parameters of batteries subjected to thermal impedance measurement

In order to apply constant heat flow to the surface of the batteries, a heating band made of Ni-Fe alloy with total resistance around 5 Ω and negligible change of this value over experimental temperature range has been tightly winded around the battery as shown in Fig. 2.

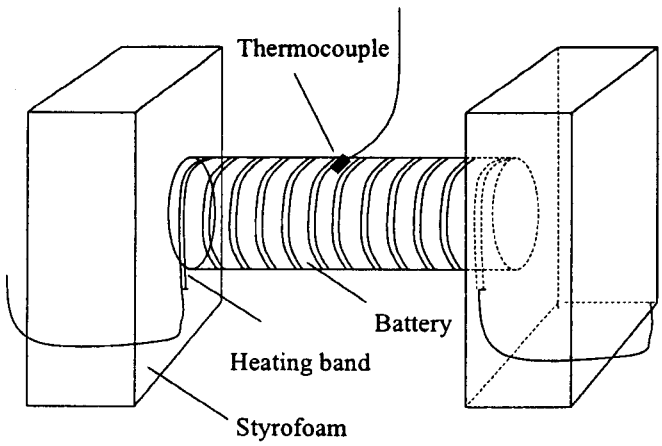

Fig. 2
Experimental set-up for thermal impedance measurement on a cylindrical battery using external heating coil for generating heat pulse

Very thin contact wire was soldered onto the heating band to provide high electric conductivity but only very low stray thermal conductivity. Both ends of contact wire were connected to the positive and the negative terminals of the BPS 1000FL. Thermocouple was fixed at the middle of the battery hight, so that it touches the surface of battery but not the heating band. Reading from thermocouple was performed by the BP1000FL and transmitted to the control PC. Battery was compressed between two plates of thermal insulator (porous polystyrene) minimizing heat conduction along battery axis and through its sides. To increase heat transfer from battery surface thereby decreasing the largest thermal time-constant of the system, 2W CPU-cooler fan was placed 1 cm from the battery to provide convection cooling. Experiments were performed in an incubator at 20°C with average temperature fluctuation 0.05°C.

Before each measurement the resistance of the coil was measured at 1kHz frequency using impedance measuring capabilities of the BPS 1000FL. With the exact value of resistance, the amount of current to apply heat pulse of 1W to the surface of the cell was calculated. The current was applied to the heating band with rise time 40 μs. Temperature response have been measured with sampling rate δt=200ms during period of Δt=1000 second. Calculations of impedance spectra were performed automatically by the BPS 1000FL control software using algorithm described in section 1. Parameters k_i were found by linear fit to 8 exponents with time-constants t_i logarithmically selected between $f_{max}=1/\delta t$ and $f_{min}=1/\Delta t$. Fit was performed using the normal equations employing Gauss-Jordan elimination method [20].

5. Results and discussion

Thermal impedance of the heating coil used for the subsequent experiments has been measured from 0.1 Hz to 1mHz in order to obtain the specific heat capacity of the coil which will be used for correction of battery data. Heat pulse of 0.5W has been applied to the coil for 1000 seconds. Temperature transient data have been converted to thermal impedance spectrum as described above. Resulting thermal impedance spectrum together with the fit obtained using Eqn. 1 are shown in Fig. 3.

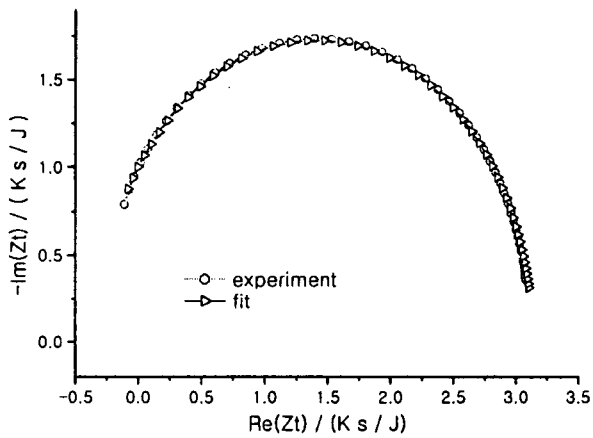

Fig.3
Thermal impedance spectrum of heating coil, measured in frequency range between 0.2 Hz and 1mHz. The fit line corresponds to thermal impedance function for the model described by Eqn. 1

The MEISP non-linear least squares fitting software developed by Kumho Petrochemical Co., Ltd. has been used for analysis of the spectra. A good fit of the spectrum by thermal impedance function indicates correctness of chosen thermal equivalent circuit model. Thermal capacity of coil obtained by the fit is 4.12 J/K.

In order to separate influence of the battery casing from the thermal behavior of electrode stack, thermal impedance spectrum of empty casing has been measured. Thermal capacity C_c of the casing together with the heating coil is found by the fit of the spectrum as 13.74 J/K.

Thermal impedance spectrum of Panasonic battery has been measured in a wide frequency range from 0.1 Hz to 100 μHz to check validity of the proposed thermal model and to obtain thermal capacity and thermal conductivity of the battery. Resulting temperature transient is shown in Fig. 4 and impedance spectrum together with model fit is shown in Fig. 5 as complex plot.

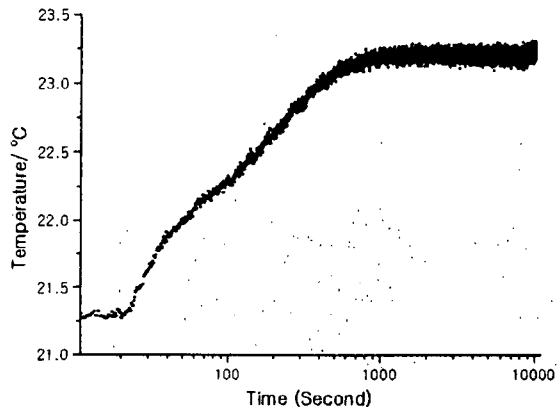

Fig.4
Temperature transient in response to 1W heat pulse applied to surface of the Panasonic Li-ion battery

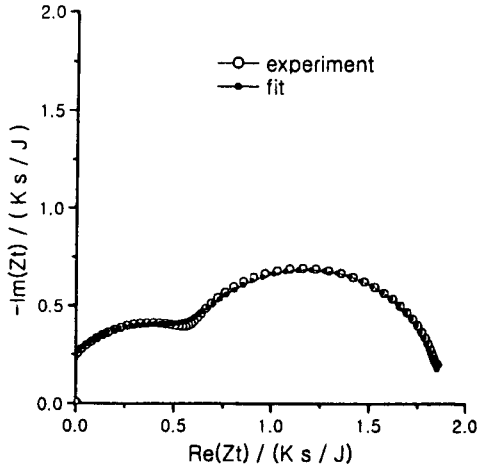

Fig.5
Thermal impedance spectrum of the Panasonic Li-ion of battery in fully charged state, measured between 0.1Hz and 100μHz. The fit line corresponds to the thermal model described by Eqn. 5 with parameter values given in Table 2

Two semicircles are visible on the plot. The depressed semicircle found in the high-frequency part corresponds to thermal capacity of battery casing in parallel with thermal resistance between the casing and the electrode stack. The semicircle is depressed by parallely placed thermal resistance of the electrode stack. The low frequency semicircle corresponds to thermal capacity of the electrode stack parallel with the thermal resistance of interfacial cooling.

The parameters of thermal model were obtained by fitting the spectrum to thermal impedance function in Eqn. 5. Casing capacity C_c obtained above has been used as fixed parameter in the fit. Good fit result indicates that proposed thermal model satisfactory describes thermal behavior of cylindrical Li-ion battery. All parameters resulting from the fit are given in Table 2.

Manufacturer	R_{ser} (K / W)	R_{rc} (K / W)	C_c (J/K)	R_c (K / W)	C_T (J/K)	R_T(K / W)
Moly Energy	-0.05	2.49	13.47	0	61.5	2.80
Panasonic	-0.1	1.98	13.74	0.90	58.4	1.78
Hitachi	-0.05	3.23	13.74	1.01	37.68	0.86
Samsung	-0.02	1.94	13.74	0	76.73	2.07

Table 2
Thermal equivalent circuit parameters obtained by fitting the thermal impedance spectra of the Li-ion batteries (Fig. 6) to thermal model in Fig. 1 described by Eqn. 5

As expected, thermal resistance of the thermocouple introduces delay in temperature onset and is therefore represented as negative resistance in thermal equivalent circuit. Thermal capacity of the metal casing is found to be responsible for 1/4 of the total thermal capacity. A better thermal contact between casing and the electrode stack can be important for improving

the heat dissipation from battery, since the thermal resistance R_c between the casing and the stack is found to be 1/3 of the total thermal resistance of battery. Thermal resistance at the battery surface due to radiation and convection cooling R_{rc} is the largest bottleneck in battery heat dissipation in spite of air circulation with fan. However, other contributions to total thermal impedance are of the same order of magnitude. In case of active cooling with water, considered for high-power applications such as electric vehicles, the thermal resistance of the electrode stack can become dominant.

Specific values of thermal parameters have been calculated using information about battery dimensions and weight in Table 1 using Eqn. 4. To calculate specific capacity of the casing, thermal capacity of the coil was subtracted, and weight of casing 8.9 gm was used. All specific values are given in Table 3.

Manufacturer	h_{RC} (W / K m^2)	c_C (J/K gm)	h_C (W / K m^2)	c_T (J/K gm)	κ_T (W / K m)
Moly Energy	109.3	1.1	-	1.8	0.9
Panasonic	137.1	1.1	302.1	1.9	1.4
Hitachi	84.5	1.1	269.3	1.2	2.8
Samsung	140.2	1.1	-	2.4	1.2

Table 3

Heat transfer coefficients, specific heat and thermal conductivity of cylindrical Li-ion batteries, obtained by fit of their thermal impedance spectra to thermal impedance function in Eqn. 5 corresponding to the thermal model given Fig. 1. Specific values are obtained using conversion equations given in Eqn. 4

Specific thermal capacity of the electrode stack with value of 1.9 J/K gm is noticeably higher than that of Sony battery previously reported as 1.07 J/K gm in [9]. Thermal capacity of the casing was not separately considered in this paper. Thermal conductivity of the electrode stack perpendicular to the electrode surface is found to be 1.4 W/K m, which is almost 5 times larger than that for Li-polymer battery, calculated in [4] on basis of known thermal conductivity of component materials. This considerable difference probably arises, apart from use of liquid electrolyte, from the fact that the winded electrode stack is used in commercial batteries (both cylindrical and prismatic), differing from the parallel electrode assumption used in the calculations. Winded electrode stack design results in thermal conduction pathways in radial direction through highly thermally conductive current collectors. The presence of such unaccounted thermal pathways can explain a much higher average thermal conductivity, found in experiment. Obtained value for surface cooling heat transfer coefficient of 137 W/K m^2 is rather high compared to 25, usually assumed for radiation and active convection cooling [4], probably due to close placement of the fan to the surface.

Thermal impedance spectra were measured on fully-charged Li-ion batteries manufactured by Panasonic, Hitachy, Moly Energy, and Samsung in frequency range from 0.1 Hz to 1mHz. Fig. 6 shows a comparison of the thermal impedance spectra of all batteries used in the experiment.

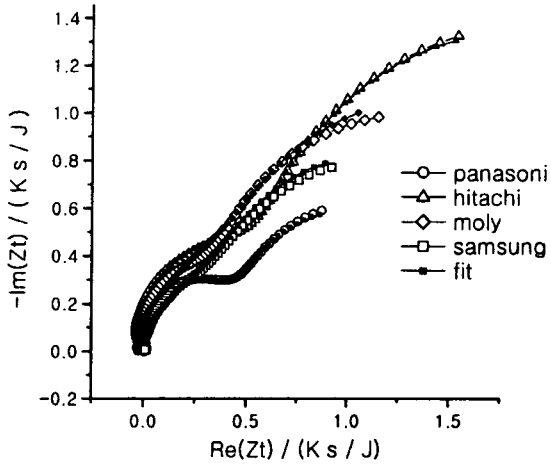

Fig 6
Comparison of thermal impedance spectra of Panasonic, Moly Energy, Hitachi, and Samsung Li-ion batteries measured between 0.1Hz and 1mHz. The fit lines correspond to thermal model described by Eqn. 5 with parameter values given in Table 2.

It can be seen that the spectra are distinctly different, in spite of the similar chemistry of batteries. This observation highlights the importance of considering the thermal properties, characteristic to each particular manufacturing technology, in designing the heat management of large battery packs with high power capabilities.

The obtained part of the low-frequency semicircle was sufficient to determine the thermal capacity of tested batteries. In order to obtain thermal parameters, the spectra have been fitted to the thermal impedance function in Eqn. 5. Resulting values of the thermal equivalent circuit elements are shown in Table 2 and specific values in Table 3.

An interesting difference is observed for Moly and Samsung batteries compared to Panasonic and Hitachi batteries. Later two batteries have noticeable thermal resistance R_c between the casing and the electrode stack, while in the case of first two batteries this resistance is negligible. Absence of close mechanical contact between the electrode stack and the casing could be the reason for this additional thermal resistance. Such loose contact should obviously be avoided to improve the protection from battery overheating. The lowest specific thermal capacitance is observed for the Hitachi battery, which also has the lowest electric capacity as shown in Table 1. The increase of electric capacity in battery design is probably related to adding more components with high thermal capacity. The electrode stack of Hitachi battery also has the highest thermal conductivity among all measured batteries. These two properties could be due to a relatively larger contribution of electrolyte to the total weight of battery.

In order to find how sensitive thermal properties of a Li-ion battery are with respect to state of charge, thermal impedance spectra of Panasonic Li-ion battery were obtained at different states of charge. The battery was fully charged and then subjected to a repetitive sequence of discharge at 5h rate for 1 hr, relaxation for 30 min and impedance spectrum measurement until it was fully discharged. Fig. 7 shows the impedance spectra obtained at different states of charge.

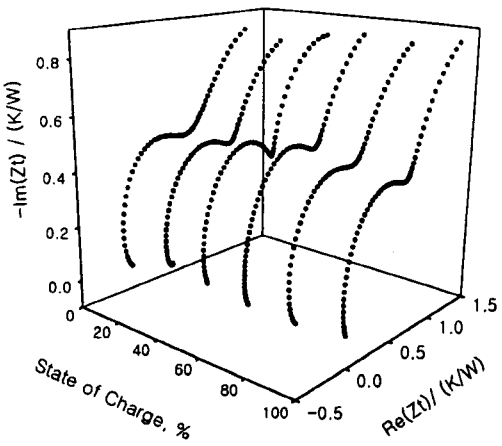

Fig. 7

Three-dimensional plot representing the dependence of impedance spectra of the Panasonic battery on the state of charge. Impedance spectra are obtained in frequency range from 0.1 Hz to 1mHz. State of charge is ranging from discharged state (0%) to fully charged state (100%).

It can be seen that thermal properties of Li-ion battery are practically independent from state of charge. The slight increase of the size of the semicircle in the high-frequency region with increasing state of charge indicates reduction of average thermal conductivity of electrode stack. Thermal capacitance of the battery remains unchanged during the discharge of battery as can be seen from the unchanged semicircle in the low-frequency region of the thermal impedance plot.

Thermal properties obtained by thermal impedance measurement can be used for simulating battery response to application of internal heat which can arise during battery operation in high-power applications. Simulation can be easily performed using equivalent circuit approach adapted earlier to analyze the thermal impedance spectra. For this purpose the equivalent circuit in Fig. 1 is modified by adding heat sources to each node of the transmission line representing cylindrical electrode stack, as shown in Fig. 8.

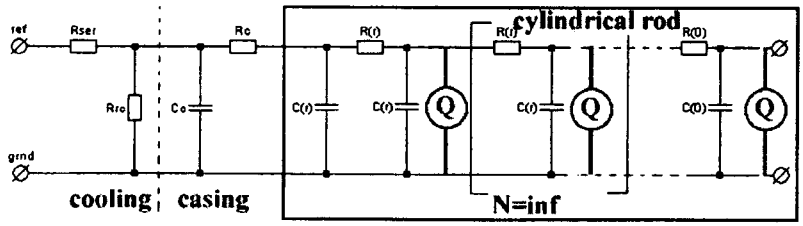

Fig. 8
Thermal equivalent circuit corresponding to cylindrical battery self-heated in its volume under radiation cooling condition

Here the values of heat sources, capacitors and resistors at each node are depending on the node number in correspondence to cylindrical configuration of electrode stack as given in Eqn. 11.

$$Q(i) = \frac{Q_{tot}}{N^2} \cdot (2 \cdot i + 1)$$

$$C(i) = \frac{C_{tot}}{\hat{} } \cdot (2 \cdot i + 1)$$

$$R(i) = R \cdot \left[\ln\left[\frac{(i+1)}{} \right] \right]$$

Eqn. 11

Here N is total number of cylindrical slices representing electrode stack. Node numbering starts from center of the battery.

Calculation of temperature response can be performed in electric circuit simulator such as freely available SPICE [21]. In the simulation current sources are used as electric equivalent of heat sources, and voltage as electric equivalent of temperature. In order to investigate differences between internal and external increase of temperature during high power operation we calculated a temperature response of Panasonic Li-ion battery to internal heating amounting to 20W, similar to heat which would develop inside the battery during 3C discharge. Results are shown in Fig. 9

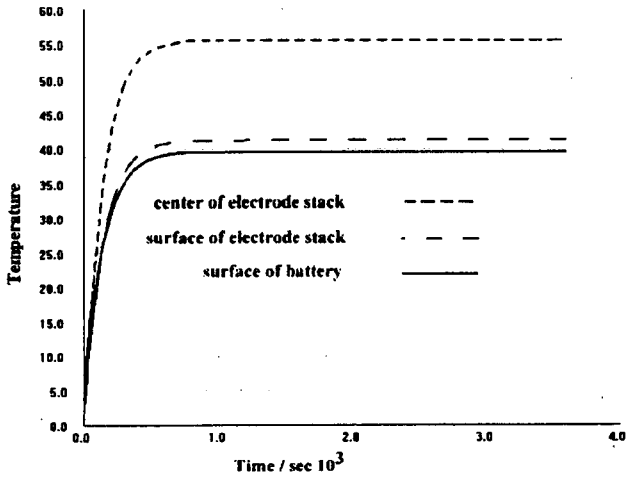

Fig. 9

Temperature response of Panasonic Li-ion battery to 20W internal heating pulse under circulation cooling conditions. Temperature dependence on time is calculated using thermal equivalent circuit in Fig. 8 and thermal properties obtained by thermal impedance measurement, listed in Table 2

It can be seen that significant difference between temperature in the center of battery and its surface develops during heating. This difference has to be accounted for to prevent damage due to overheating of battery materials.

6. Conclusions

In this work we demonstrated a possibility of simultaneous measurement of thermal capacity and thermal conductivity of cylindrical batteries by analysis of thermal pulse response. Derivation of thermal impedance spectrum from temperature response transient by carrier-function Laplace transform was described. Methods was applied to thermal impedance measurements on the Li-ion batteries produced by Panasonic, Moly Energy, Hitachi, and Samsung. Considerable differences in the thermal properties have been observed in spite of the similar basic chemistry and design of the batteries.

The frequency domain thermal impedance function for cylindrical battery was derived and applied to the analysis of thermal impedance spectra. Specific thermal conductivities and

capacities were calculated for all measured batteries by fitting experimental thermal impedance spectra to theoretical function. These values can be used further in thermal modeling of batteries, which is applied for design of high-power systems such as electric vehicles. A large thermal resistance between the casing and the electrode stack was detected for Panasonic and Hitachi batteries, indicating that closer fitting of the electrode stack can improve the of high-power capabilities of these batteries.

Dependence of the thermal properties on the state of charge was studied on Panasonic Li-ion battery. It was found that thermal impedance spectrum remains almost unchanged during battery discharge. A slight increase of thermal conductivity with state of charge was observed.

Obtained data was used to simulate a response of the battery to internal heating during discharge. It is found that temperature inside the battery is by one-third larger that on its surface. This observation has to be considered to prevent damage by overheating.

References

1 Takeshi Miyamoto, proceedings of 13th international electric vehicle symposium, 1 (1996) 37
2 C.R.Pal and J.Newman, J.Electrochem.Soc.,142 (1995) 3274
3 M.Verbrugge, AlChE J., 41 (1995) 1550
4 L.Song and J.W. Evans, J.Electrochem.Soc., 147 (2000) 2087
5 Y.Chen and J.W.Evans, J. Electrochem.Soc. 140 (1993) 1833
6 C.R.Pal and J.Newman, J.Electrochem.Soc.,142 (1995) 3282
7 L.Song, Y. Chen and J.Evans, J.Electrochem.Soc. 144/11 (1997) 3797
8 J.Song, J.Evans, J.Electrochem.Soc., 146/3 (1999) 869
9 J.S.Hong, H.Maleki, S.Al Hallaj, L. Redey, and J.R.Selman, J.Electrochem.Soc., 145 (1998) 1489
10 S.Al Hallaj, J.Prakash, J.R.Selman, J. Power Sources, 87 (2000) 186
11 M. Carmona, S. Marco, J. Palacin, and J. Samitier, IEEE transactions on comp. and pack. tech., 22/2 (1999) 238
12 E.Delacre,D.Defer, B.Duthoit, ASME, 1 (2000) 414
13 J.S. Turner, J. therm. Biol. 19 (1994) 237
14 H.S.Carslaw and J.C. Jaeger, Conduction of heat in solids, second edition, Oxford University Press, 1959
15 T.Jacobsen and K.West, Electrochimica Acta, 40/2 (1995) 255
16 A.A.Pilla, J.Electrochem.Soc. 117 (1970) 467
17 US Patent N5794008
18 J.Ye, K.Doblhofer, J.Electroanal.Chem., 272 (1989) 29
19 E.Barsoukov, J.H.Jang, H.Lee, submitted to Electrochem. Acta (2001)
20 Numerical Recepies in fortran, second edition, W.H.Press, S.A.Teukolsky, W.T.Vetterlin, B.P. Flannery, Cambridge University Press, 1992, chap. 15.4

21 L. W. Nagel, "SPICE2: A Computer Program to Simulate Semiconductor Circuits', ERL Memo No. ERL-M520", University of California, Berkeley, USA, 1975